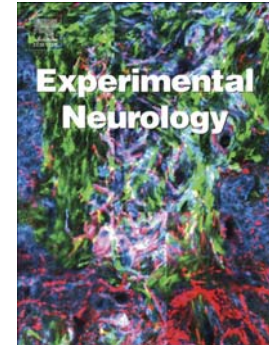


Accepted Manuscript



A β -amyloid peptide-induced cognitive impairment and its reversal by a novel β -secretase inhibitor in a mouse model of Alzheimer's disease

Sam A. Deadwyler, Robert E. Hampson, Dong Song, Ioan Opris, Greg A. Gerhardt, Vasilis Z. Marmarelis, Theodore W. Berger

PII: S0014-4886(16)30149-2
DOI: doi: [10.1016/j.expneurol.2016.05.031](https://doi.org/10.1016/j.expneurol.2016.05.031)
Reference: YEXNR 12308

To appear in: *Experimental Neurology*

Received date: 1 December 2015
Revised date: 21 May 2016
Accepted date: 23 May 2016

Please cite this article as: Deadwyler, Sam A., Hampson, Robert E., Song, Dong, Opris, Ioan, Gerhardt, Greg A., Marmarelis, Vasilis Z., Berger, Theodore W., A β -amyloid peptide-induced cognitive impairment and its reversal by a novel β -secretase inhibitor in a mouse model of Alzheimer's disease, *Experimental Neurology* (2016), doi: [10.1016/j.expneurol.2016.05.031](https://doi.org/10.1016/j.expneurol.2016.05.031)

This is a PDF file of an unedited manuscript that has been accepted for publication. As a service to our customers we are providing this early version of the manuscript. The manuscript will undergo copyediting, typesetting, and review of the resulting proof before it is published in its final form. Please note that during the production process errors may be discovered which could affect the content, and all legal disclaimers that apply to the journal pertain.

A Cognitive Prosthesis for Memory Facilitation by Closed-loop Functional Ensemble Stimulation of Hippocampal Neurons in Primate Brain

Sam A. Deadwyler, *WFUHS*, Robert E. Hampson, *WFUHS*, Dong Song, *USC*, Ioan Opris *WFUHS*, Greg A. Gerhardt, *UKY*, Vasilis Z. Marmarelis, *USC*, and Theodore W. Berger, *USC*

Abstract—Very productive collaborative investigations characterized how multineuron hippocampal ensembles recorded in nonhuman primates (NHPs) encode short-term memory necessary for successful performance in a delayed match to sample (DMS) task and utilized that information to devise a unique nonlinear multi-input multi-output (MIMO) memory prosthesis device to enhance short-term memory in real-time during task performance. Investigations have characterized how the hippocampus in primate brain encodes information in a multi-item, rule-controlled, delayed match to sample (DMS) task. The MIMO model was applied via closed loop feedback micro-current stimulation during the task via conformal electrode arrays and enhanced performance of the complex memory requirements. These findings clearly indicate detection of a means by which the hippocampus encodes information and transmits this information to other brain regions involved in memory processing. By employing the nonlinear dynamic multi-input/multi-output (MIMO) model, developed and adapted to hippocampal neural ensemble firing patterns derived from simultaneous recorded multi-neuron CA1 and CA3 activity, it was possible to extract information encoded in the Sample phase of DMS trials that was necessary for successful performance in the subsequent Match phase of the task. The extension of this MIMO model to online delivery of electrical stimulation patterns to the same recording loci that exhibited successful CA1 firing in the DMS Sample Phase provided the means to increase task performance on a trial-by-trial basis. Increased utility of the MIMO model as a memory prosthesis was exhibited by the demonstration of cumulative increases in DMS task performance with repeated MIMO stimulation over many sessions. These results, reported below in this article, provide the necessary demonstrations to further the feasibility of the

MIMO model as a memory prosthesis to recover and/or enhance encoding of cognitive information in humans with memory disruptions resulting from brain injury, disease or aging.

***Index Terms*—Closed-loop, neural prosthesis, memory, hippocampus, ensemble, electrical stimulation, nonlinear model**

INTRODUCTION

Encoding of memory by brain systems has long been one of the major interests of neuroscience research, since this process allows temporal bridging between events that occur at different times, as well as expectation of future circumstances based on accurate recall of prior experiences (Eichenbaum and Fortin, 2009). Effective memory encoding requires detection, categorization and recognition, in order to allow adequate performance in a number of different circumstances (Davachi, 2006) as indicated most dramatically by Alzheimer’s disease in which total memory loss leads to incapacitation and helplessness (Gold, Smith, Bayley, Shrager, Brewer, Stark, Hopkins, and Squire, 2006). The brain structure most intricately involved in this process is the hippocampus, which exists in all mammalian species and is capable of long-term retention of goal-directed objectives (Eichenbaum, Yonelinas, and Ranganath, 2007; Klausberger and Somogyi, 2008; Manns, Hopkins, Reed, Kitchener, and Squire, 2003; Squire, Wixted, and Clark, 2007). Development of new technologies and brain-behavior assessments has allowed progressive insight into the process of memory formation and retrieval in hippocampus (Eichenbaum and Cohen, 2001; Quirk, Muller, Kubie, and Ranck, Jr., 1992; Ross and Slotnick, 2008; Rutishauser, Mamelak, and Schuman, 2006; Wais, Wixted, Hopkins, and Squire, 2006; Winters and Bussey, 2005). This has progressed to the extent of making it possible to formulate and test a “device” that can substitute for these functions when they are compromised by damage or disease (Berger and Glanzman, 2005) in the same manner as other neural prostheses (Berger, Ahuja, Courellis, Deadwyler, Erinjippurath, Gerhardt, Gholmieh, Granacki, Hampson, Hsaio, LaCoss, Marmarelis, Nasiatka, Srinivasan, Song, Tanguay,

and Wills, 2005;Hampson, Simeral, and Deadwyler, 2005;Song, Chan, Marmarelis, Hampson, Deadwyler, and Berger, 2007a).

In order to understand the neural basis of memory in hippocampus several features of both the context in which encoding occurs as well as the functional aspects of simultaneous multineuron firing patterns, must be identified, interpreted and manipulated, which has been one of the important objectives of the research described here. This entails integrating; 1) an effective operational mathematical model for online prediction of cell discharges in the CA1 field from simultaneously recorded firing patterns of presynaptic CA3 neurons (Marmarelis and Orme, 1993;Song *et al.*, 2007a;Song, Chan, Marmarelis, Hampson, Deadwyler, and Berger, 2009;Truccolo, Eden, Fellows, Donoghue, and Brown, 2005), together with, 2) obtaining systematic recordings of hippocampal neural ensemble activity in a behavioral task in which trial-to-trial short-term encoding of task features is required for successful performance (Deadwyler, Bunn, and Hampson, 1996;Deadwyler and Hampson, 2006). The combining of these two approaches has involved the analysis and characterization of neuronal firing patterns in CA3/CA1 hippocampal subfields repeatedly subjected to mathematical nonlinear input/output analysis (Marmarelis, 2004;Song, Chan, Marmarelis, Hampson, Deadwyler, and Berger, 2007b;Zanos, Courellis, Berger, Hampson, Deadwyler, and Marmarelis, 2008) in both rodents and nonhuman primates performing a short-term memory task (Hampson, Simeral, Berger, Song, Chan, and Deadwyler, 2011;Hampson, Song, Chan, Sweatt, Riley, Gerhardt, Shin, Marmarelis, Berger, and Deadwyler, 2012;Hampson, Song, Opris, Santos, Shin, Gerhardt, Marmarelis, Berger, and Deadwyler, 2013). The culmination of these investigations (Berger, Hampson, Song, Goonawardena, Marmarelis, and Deadwyler, 2011) demonstrated that the “firing codes” extracted online by a custom designed multi-input/multi-output (MIMO) nonlinear model, when re-injected via identical electrical stimulation patterns could 1) enhance performance by changing the strength of encoding required for the memory task and 2) recover the pharmacologically compromised operation of hippocampus by re-inserting electrically-mimicked natural codes in the same animals performing task.

In the studies reported here four additional features of the MIMO model extracted firing patterns of hippocampal neural ensembles are shown that provide further support for its application as a memory prosthesis. First, the actual basis of the utility of ensemble spatiotemporal firing patterns detected by the MIMO model is revealed in terms of the degree to which encoding of specific task events reflects the level of performance on a given trial. Second, it is shown that if given repeatedly on specified trials within the testing session, MIMO model electrical stimulation patterns also enhances performance on trials without stimulation delivered in the same sessions, and, that such enhancement persisted even after the stimulation trials were terminated in the session. Third, it has been shown that similar types of hippocampal encoding patterns exist across different animals tested in the same task. Finally, it is revealed that ensemble firing patterns extracted online by the MIMO model conform to the synchronized firing of cells in the ensemble that naturally and successfully encode task features (Hampson, Simeral, and Deadwyler, 2008). Collectively these findings support the feasibility of applying the current prosthetic device (Hampson *et al.*, 2013) to 1) repair damaged or disrupted brain-memory processes, and/or 2) enhance memory functions in circumstances where retention is weak or ineffective (Chapin, 2004; Schwartz, Moran, and Reina, 2004; Song *et al.*, 2007a; Wessberg, Stambaugh, Kralik, Beck, Laubach, Chapin, Kim, Biggs, Srinivasan, and Nicolelis, 2000).

The report below provides a detailed description of work that applied this approach to assessing hippocampal involvement in the encoding of relevant information by nonhuman primates (NHPs) engaged in a complex cognitive memory task requiring retention of several stimulus features as well as trial specific information to perform correctly, described in several prior reports (Deadwyler, Porrino, Siegel, and Hampson, 2007; Hampson, Espana, Rogers, Porrino, and Deadwyler, 2009; Hampson, Pons, Stanford, and Deadwyler, 2004; Porrino, Daunais, Rogers, Hampson, and Deadwyler, 2005).

Those results and what is presented here, show that MIMO model derived stimulation applied to hippocampal CA3&CA1 sub-regions in task performing NHPs, provides a high degree of facilitation of performance across different types of memory challenges. The MIMO model

therefore satisfies the criteria to serve as a neural prosthesis in primate brain as demonstrated extensively in multiple tests with NHPs (Hampson, Gerhardt, Marmarelis, Song, Opris, Santos, Berger, and Deadwyler, 2012; Hampson *et al.*, 2013). The results strongly indicate the potential efficacy for recovering memory based brain area dysfunction related to disease states, and/or aging in humans (Riddle and Lichtenwalner, 2007).

Methods and Procedures

Cognitive Memory Task: Four nonhuman primates (NHP) were subjects (rhesus, *Macaca mulatta*) trained for at least 2 years to perform a well-established visuospatial delayed-match-to-sample (DMS) task (Figure 1A) for juice rewards (Hampson *et al.*, 2012; Hampson, Opris, and Deadwyler, 2010; Hampson *et al.*, 2004; Hampson *et al.*, 2013; Opris, Fuqua, Huettl, Gerhardt, Berger, Hampson, and Deadwyler, 2012; Opris, Hampson, Gerhardt, Berger, and Deadwyler, 2012). All animal procedures were reviewed and approved by the Institutional Animal Care and Use Committee of Wake Forest University, in accordance with U.S. Department of Agriculture, International Association for the Assessment and Accreditation of Laboratory Animal Care, and National Institutes of Health, guidelines. Animals were seated in a primate chair with a shelf-counter in front of them facing a large display screen during task performance. Right hand position on the counter top was tracked via a UV-fluorescent reflector affixed to wrist and illuminated with a 15 W UV lamp. Hand position and movement was detected by a small LCD camera positioned 30 cm above the hand, digitized using a Plexon Cineplex scanner connected to a behavioral control computer, and displayed as a bright yellow cursor on the projection screen. Trials were initiated by the animal placing the cursor inside either a yellow circle or red square (centrally-placed) that appeared randomly on the screen which constituted the 'Start Signal' (SS) for a given trial (Figure 1). Following trial initiation by response to the SS, a single image was presented randomly as the Sample feature of the trial, to any of seven positions on the screen, constituting the 'Sample Presentation' (SP) phase of the task. Completion of the Sample phase required placement of the cursor into the displayed clip-art image, and was designated the *Sample Response* (SR). The particular shape of the SS (square or circle)

presented at trial onset, conveyed the response contingency with respect to the SP features (image type or screen position) when presented in the subsequent Match phase of the task with other distracter images following termination of the interposed variable (1-90s) Delay interval. If the SS was: 1) a yellow circle this indicated an *Object* type trial in which the SP clip-art image was to be responded to in the Match Phase irrespective of where on the screen it appeared in 7 other possible screen positions or, 2) a red square, indicating a *Spatial* type trial in which the correct response in the Match phase was to touch the same spatial location on the screen in which the SP image appeared irrespective of a) the particular clip-art image that occupied that same location, or b) where else on the screen the original SP clip-art image appeared during the Match phase.

The SR initiated the *Delay* interval phase of the trial, in which the screen was blanked for 1-90s, randomly determined on a trial-to-trial basis. The end of the Delay interval was signaled by the onset of the Match Phase (MP) of the task, consisting of the simultaneous display of 2–7 trial unique images, including the SP image, at separate randomly-selected, spatial locations on the screen. Placement of the cursor into one of the displayed images constituted the “Match Response” (MR), the final event. As stated above, selection of the correct image in the MP was dictated by the SS trial type contingency for cursor placement in the MP into either: 1) the same SP *image* no matter where located on the screen, on *Object* trials, or 2), the same Sample phase SP *screen location* (irrespective of image) on *Spatial* trials (Figure 1A). Correct MRs produced immediate delivery of a juice reward directly to the mouth via a positioned tube. Incorrect cursor placement constituted a *nonmatch-error* response and caused the screen to blank without delivery of the juice reward. Trials during the session were separated by a minimum of 10 sec. in which the SS was presented following termination of the Match phase of the prior trial. All clip-art images presented (sample and distracters) were unique for each trial in a daily session (100-150 trials), and were selected randomly from an image reservoir (n=5000) which could be updated every month (Hampson *et al.*, 2004). In the above described version of the DMS task NHPs were trained to overall performance levels of 70-75% correct on

the least difficult trials, which produced performance accuracy that systematically decreased as delays and number of images increased.

---Figure 1 goes here ---

Surgery: Animals were surgically prepared with cylinders on the skull for daily attachment of microelectrodes and manipulators into the CA1 and CA3 regions of hippocampus (Figure 1B). During surgery animals were anesthetized with ketamine (10 mg/kg), then intubated and maintained with isoflurane (1-2% in oxygen 6 l/min). Recording cylinders (Crist Instruments, Hagerstown, MD) were placed over 20 mm diameter craniotomies for electrode access (Hampson *et al.*, 2004) to stereotaxic coordinates of the Hippocampus (Figure 1) previously shown by PET imaging (Porrino *et al.*, 2005) to become activated during task performance. Two titanium posts were secured to the skull for head restraint and recording cylinders were disinfected thrice weekly with Betadine during recovery and daily following task recording.

Recording from Hippocampus: Electrophysiological procedures and analysis utilized the 64 channel MAP Spike Sorter by Plexon, Inc. (Dallas, TX). Customized tetrode arrays were manufactured specifically for recording spatially distinct locations in the CA3 and CA1 cell fields in primate hippocampus (Hampson *et al.*, 2004; Santos, Opris, Fuqua, Hampson, and Deadwyler, 2012) such that multi-cell ($n > 12$) recordings could be obtained from each anatomically distinct location. The robust Schaefer collateral projections from CA3 to CA1 insured that locations recorded from in CA3 were likely connected synaptically to the locations recorded in CA1 in each Tetrode pair positioned in the same mediolateral plane or “chip” of hippocampus in two distinct anterior/posterior locations as shown in Figures 1B & 4.

Data Analysis: Task performance was determined for each animal ($n=4$) as number of correct and incorrect responses within trial groups sorted according to duration of delay and number of images presented in the Match phase (Figures 1C,1D,1E). Number of trials were summed, and percentage of correct responses computed within sessions, with average performance

computed across a minimum of three sessions (Hampson *et al.*, 2012). Recordings of multiple neuron firings on individual trials during the Sample and Match phases of the DMS task were summed within 100 ms intervals, and averaged across trials within a session for display of mean firing rate via perievent histograms (PEHs) within both the Sample or Match task events (Figures 2,3).

Significant firing peaks were identified by an increase in firing rate (standard score: $z = [\text{peak} - \text{baseline}] / \text{standard deviation of baseline}$). Firing rates for simultaneously recorded CA1 and CA3 neurons were analyzed in 100 ms bins over ± 2.0 s relative to the time of initiation (0.0s) of the Sample and Match phases of the task. "Peak" firing rates were computed as maximum firing rate (as a sliding 3-bin mean) ± 0.5 s relative to each event, while "Baseline" firing rates were computed -2.0 to -1.0 s relative to the same event. Baseline firing ranged from 2.0-4.0 Hz depending on phase of task, with S.D.'s of 0.1-0.4 Hz; significant Peak firing was typically elevated by 1.0-2.0 Hz over baseline firing at the Sample and Match events. Standard scores were assessed for significance using the Z distribution such that $z > 3.09$ were considered significant increases over baseline ($p < 0.001$). Neurons were only included in the analysis if their firing rates increased significantly relative to pre-event (-2.0 to 0.0s) baseline levels.

The correspondence of firing between cells in different layers was tested via comparison of trial-based histograms (TBHs) spanning more than one task event within a phase to construct templates related to how the hippocampus encoded trial specific information. Perievent histograms (PEHs) demarcated firing differences for individual events and provided the basis for nonlinear model analyses of firing during particular Sample and Match events within a given trial.

MIMO Model for Extracting DMS Task-related Hippocampal Neural Activity: Prior studies in rodents showed that a multi-input/multi-output (MIMO) nonlinear dynamic model applied to spatiotemporal firing patterns of multiple recordings from rodent hippocampal CA1 and CA3 neurons was capable of extracting specific patterns related to successful performance of a

nonmatch to sample memory task, which could then be administered to the same locations as patterns of electrical pulses to facilitate and recover performance (Berger *et al.*, 2011; Hampson *et al.*, 2012; Hampson, Song, Chan, Sweatt, Riley, Goonawardena, Marmarelis, Gerhardt, Berger, and Deadwyler, 2012; Hampson *et al.*, 2013). The same MIMO model was applied to hippocampal recordings in NHPs to assess the spatiotemporal nonlinear dynamics underlying multi-neuron spike train transformations in order to predict CA1 output firing patterns from input patterns of CA3 neural activity, via underlying Shaffer collateral synaptic connectivity (Deguchi, Donato, Galimberti, Cabuy, and Caroni, 2011; Klausberger *et al.*, 2008). The MIMO version of the model applied here was derived from the data recorded by the multiple tetrode ceramic electrode array (MEA) probes in NHPs performing the DMS task described in Figure 1 (Hampson, Song, Chan, Sweatt, Fuqua, Gerhardt, Shin, Marmarelis, Berger, and Deadwyler, 2012).

RESULTS

MIMO Model Produces Successful Memory Facilitation in Hippocampus of Primate Brain

One of the next steps in the development of the memory prosthesis for primate brain was to make sure that NHP hippocampal activity could be accessed and modulated in the same manner as prior investigations in the rodent. This was accomplished by designing and implementing arrangements of tetrode arrays placed simultaneously in CA1 and CA3 in NHPs prior to daily task performance (Santos *et al.* 2012). Figure 1 shows results from adult male rhesus macaques (n=4) trained to perform the DMS task (Hampson *et al.*, 2013; Opris *et al.*, 2012). As described above, NHPs were rewarded for the appropriate SP selection in the subsequent Match phase of the same trial.

Hippocampal Neural Activity Related to Information Encoding in the Sample Phase

For validation of hippocampal participation in the DMS task it is necessary that the recorded CA3 and CA1 neuron firing during the Sample phase of the DMS task represent the degree of image or spatial encoding required for accurate recall and selection of the proper target in the Match phase after the interposed variable delay (Figure 1). Figure 2 illustrates firing of a single ensemble of fifteen CA1 (n=6) and CA3 (n=9) hippocampal neurons recorded from an NHP during performance of DMS Object and Spatial Trials. It is clear that the spatiotemporal distribution of firing across neurons was different for correct Object vs. correct Spatial trials. In this ensemble, Object trials produced increased firing not only at the labeled DMS events, but also between SP-SR and MP-MR events, while Spatial trials primarily exhibited increased firing at the SP, SR, MP and MR events. Error trials yielded not only less firing overall, but also decreases in event-synchronized ensemble firing across neurons.

---Figure 2 goes here ---

Figure 3A shows that CA1 (n=431) and CA3 (n=801) neurons, recorded across multiple ensembles/recording sessions for all animals (n=4 NHPs), exhibited significantly increased peaks in average firing rate ($p < 0.001$) during the 3 critical events in the Sample phase: Trial Start signal *Strt* (*SS*), Sample Image Presentation-*SP*; and Response to Sample image-*SR*. An important feature regarding this phase of the task in addition to the three distinct events for encoding Sample information was the significantly elevated overall firing above baseline levels (Figure 4A) for neurons in CA1 and CA3 in a manner that was different with respect to a) the type of trial presented (“Start” in Figure 4A) and b) subsequent implications for correct or error trials. Figure 4B shows this differentiation for all 4 possible outcomes with respect to trial type and performance. What is very important is the fact that mean firing rates in CA1 and CA3 were significantly different with respect to the *Strt* (*SS*), *SP* and *SR* events on Object vs. Spatial trials (Figure 3B).

---Figure 3 goes here ---

Hippocampal Neural Activity During Target Selection in the Match Phase

The basis for effective encoding by CA1 and CA3 neural activity in the Sample phase of successful trials, culminated in the selection of either the same Sample image (Object trial) or the same Sample screen location (Spatial trial) after the interposed variable delay period in the Match phase of the DMS task. Figures 4A&B show the average firing rates of the same CA3 and CA1 neurons displayed in Figures 3A&B for events in the Match phase of the same trials. Firing is demarcated into discharges during: 1) the match screen image presentation (MP) and 2) match response (MR) via movement of the cursor into one of the selected Sample features, The MR determined a correct or error trial with respect to correspondence with previously presented information in the Sample phase of the same trial (Figure 3A). The average firing rates of CA1 and CA3 neurons associated with the MP and MR events on both types of trial (Object and Spatial) is shown in Figure 3A which reveals that the increase in firing at the onset of the match phase (MP) continued through completion of the MR. Average peak firing rates in CA1 and CA3 across all animals during the same events is shown in Figure 4B in which discharges during the MR were distinctly different for correct vs. error performance on both Object and Spatial trials, with CA1 neurons exhibiting higher rates than CA3 neurons.

---Figure 4 goes here ---

MIMO Model Extraction of Successful Hippocampal Processing of Sample Information

The MIMO model was applied to the same form of hippocampal neuron firing extracted during the Sample phase of the DMS task as shown in Figures 1-4. The MIMO model shown in Figure 5 provided identification and extraction of spatio-temporal firing patterns from neurons recorded in CA3 that were synchronized with neurons recorded in CA1 (Berger *et al.*, 2011;Marmarelis, 2004;Marmarelis and Berger, 2005;Marmarelis, Shin, Song, Hampson, Deadwyler, and Berger, 2011;Song *et al.*, 2009). These patterns were formulated into a nonlinear MIMO model which decomposed into a series of multi-input, single-output (MISO) models with physiologically

identifiable patterns described in Figure 5. The model describes the temporal relationship of CA1 neural spike events to CA3 neural spikes that occurred previously both within and across all spike trains recorded, in order to determine the sequence of synaptically related CA1 spikes constituting hippocampal outputs.

---Figure 5 goes here ---

Analyses included extraction of first, second and third order temporal firing recorded by dual tetrodes inserted into both hippocampal layers over multiple recording sessions in order to extract relevant spatiotemporal patterns of CA3-to-CA1 activity associated with successful Sample selection during the Match phase of the task. The model defined inputs as firing from neurons in CA3 and outputs as temporally associated firing of CA1 neurons in similar longitudinal anatomic locations. This determined the nature of the output patterns extracted by the MIMO model and allowed predictions of CA1 firing related to successful performance that could be monitored online from tetrodes in CA3 during the Sample phase of the task (Figure 6). With this arrangement it was possible to detect via CA3 firing patterns when successful trials were about to be completed prior to appropriate target selection (MR) in the Match phase of the same trial. As such, this allowed delivery of electrical stimulation in similar patterns to the same CA1 electrode locations during the Sample phase, but on trials in which such prior appropriate CA3 activity did not occur, and this augmented performance in this memory-dependent task (Figure 7).

---Figure 6 goes here ---

MIMO Model Extraction of Trial-Specific CA1 Neuron Firing Patterns Related to CA3 Inputs

Prior investigations applying MIMO model-derived patterns of electrical stimulation pulses to the hippocampus in rodents enhanced performance of a short-term memory task (Berger *et al.*, 2011; Hampson *et al.*, 2012). The same approach was employed in DMS-trained NHPs in which simultaneous spatiotemporal recordings from CA3 and CA1 neurons were used to construct

MIMO models capable of predicting CA1 firing from online-monitored CA3 inputs on the same trials, shown in Figure 6. These patterns were derived specifically from simultaneous CA3 neuron firing in the Sample phase related to Strt (SS), SP and SR task events shown in Figs 3&4. Figure 6 shows averaged PEHs depicting predicted CA1 neural as 'heat map displays' averaged over the respective trial types shown in a single session. The MIMO model (Figure 5) was used to predict specific CA1 firing patterns from the same animal that coincided with CA3 neuron firing during the Sample phase of the task on both Object and Spatial trials. Representative Object and Spatial trial firing patterns for 'predicted' CA1 output patterns represented in Figure 6 show reciprocity in the patterns corresponding to strong encoding (correct trial left) for one trial type with the weak (error trial right) coding reflecting features of the opposite trial type.

---Figure 7 goes here ---

Figure 7 demonstrates the effectiveness of the MIMO derived CA1 stimulation patterns delivered to four NHPs in which facilitation of performance occurred primarily on trials with increased difficulty with respect to both length of delay (inset graphs) and b) number of distracter images (main graphs). Delivery of MIMO strong code stimulation patterns facilitated performance in each NHP subject, however the degree of performance improvement was greater on trials with either: 1) increased duration of delay (delay: $F(3,1682) = 7.04, p < 0.001$) and/or, 2) increase in the number of distracter images (number of images: $F(5,1682) = 5.13, p < 0.001$). These changes produced by the delivery of strong code stimulation during the Sample phase of the task resembled performance increases that occurred on trials in prior sessions from which the MIMO model extracted the strong codes from the same cells (Figure 7 - by delay: $F(3,3106) = 7.67, p < 0.001$, or by number of images: $F(5,3106) = 9.04, p < 0.001$). In addition, even though performance on stimulation trials was proportionately decreased as a function of increased trial difficulty, the reduction was less than on trials of the same type that were not stimulated.

SUMMARY: THE MEMORY PROSTHESIS - DEVELOPING STATUS

The above demonstrations of the effectiveness of the MIMO model for deriving and restoring memory in NHPs performing a complex cognitive task provide the basis for the extension of this model to human patients with memory disorders that result from head injury or chronic deterioration such as Alzheimer's disease. Since these applications of the MIMO model were effective across different NHPs, the technique was effective in resolving differences between subjects by 1) applying conformal electrodes to the same specific brain regions, and 2) extracting effective multineuron spatiotemporal firing patterns from these areas in each subject. This provides the necessary control for applying the MIMO model to human patients with differing degrees of memory impairment since each type of deficit can be facilitated by enhancing memory encoding in non-affected regions. A major benefit of the continued development of this Prosthesis model is the possibility that it could be applied to deficiencies in different brain regions as long as electrode detection of neural activity is possible in the regions related to those types of cognitive deficits. The current status of the MIMO model presented here, in which encoding of information within the hippocampus of several different NHPs performing a memory task was improved, provides the basis for extending this prosthesis to humans to restore neuronal encoding and retrieval in disease or injury contexts in which memory failure has been determined as a major life-style impairment.

ACKNOWLEDGEMENTS

The authors acknowledge the technical assistance of Joshua Long, Joseph Noto, Christina Dyson, Brian Parrish, Jeff Atwell, Michael Todd, and Lucas Santos, Ph.D. This work was supported by DARPA REMIND (N66001-09-C-2080 to S.A.D., N66001-09-C-2081 to T.W.B), and RAM (N66001-14-C-4016) Programs, G. Ling and J. Sanchez, Program Managers.

LITERATURE CITED

1. Berger, T.W., Ahuja, A., Courellis, S.H., Deadwyler, S.A., Erinjippurath, G., Gerhardt, G.A., Gholmieh, G., Granacki, J.J., Hampson, R., Hsaio, M.C., LaCoss, J., Marmarelis, V.Z., Nasiatka, P., Srinivasan, V., Song, D., Tanguay, A.R., Wills, J., 2005. Restoring lost cognitive function. *IEEE Eng Med. Biol. Mag.* 24, 30-44.
2. Berger, T.W., Glanzman, D.L., 2005. *Toward replacement Parts for the Brain*. MIT Press, Cambridge, MA.
3. Berger, T.W., Hampson, R.E., Song, D., Goonawardena, A., Marmarelis, V.Z., Deadwyler, S.A., 2011. A cortical neural prosthesis for restoring and enhancing memory. *Journal of Neural Engineering* 8, 046017.
4. Chapin, J.K., 2004. Using multi-neuron population recordings for neural prosthetics. *Nat. Neurosci.* 7, 452-455.
5. Davachi, L., 2006. Item, context and relational episodic encoding in humans. *Current Opinion in Neurobiology* 16, 693-700.
6. Deadwyler, S.A., Bunn, T., Hampson, R.E., 1996. Hippocampal ensemble activity during spatial delayed-nonmatch-to-sample performance in rats. *J. Neurosci.* 16, 354-372.
7. Deadwyler, S.A., Hampson, R.E., 2006. Temporal coupling between subicular and hippocampal neurons underlies retention of trial-specific events. *Behavioral Brain Research* 174, 272-280.
8. Deadwyler, S.A., Porrino, L., Siegel, J.M., Hampson, R.E., 2007. Systemic and nasal delivery of orexin-A (Hypocretin-1) reduces the effects of sleep deprivation on cognitive performance in nonhuman primates. *J. Neurosci.* 27, 14239-14247.
9. Deguchi, Y., Donato, F., Galimberti, I., Cabuy, E., Caroni, P., 2011. Temporally matched subpopulations of selectively interconnected principal neurons in the hippocampus. *Nat. Neurosci.* 14, 495-504.
10. Eichenbaum, H., Cohen, N.J., 2001. *From Conditioning to Conscious Recollection: Memory Systems of the Brain*. Oxford University Press, New York.
11. Eichenbaum, H., Fortin, N.J., 2009. The neurobiology of memory based predictions. *Philos. Trans. R. Soc. Lond B Biol. Sci.* 364, 1183-1191.
12. Eichenbaum, H., Yonelinas, A.P., Ranganath, C., 2007. The medial temporal lobe and recognition memory. *Annu. Rev. Neurosci.* 30, 123-152.

13. Gold, J.J., Smith, C.N., Bayley, P.J., Shrager, Y., Brewer, J.B., Stark, C.E., Hopkins, R.O., Squire, L.R., 2006. Item memory, source memory, and the medial temporal lobe: concordant findings from fMRI and memory-impaired patients. *Proc. Natl. Acad. Sci. U. S. A* 103, 9351-9356.
14. Hampson, R.E., Espana, R.A., Rogers, G.A., Porrino, L.J., Deadwyler, S.A., 2009. Mechanisms underlying cognitive enhancement and reversal of cognitive deficits in nonhuman primates by the ampakine CX717. *Psychopharmacology (Berl)* 202, 355-369.
15. Hampson, R.E., Gerhardt, G.A., Marmarelis, V.Z., Song, D., Opris, I., Santos, L., Berger, T.W., Deadwyler, S.A., 2012. Facilitation and restoration of cognitive function in primate prefrontal cortex by a neuroprosthesis that utilizes minicolumn-specific neural firing. *J. Neural Eng* 9, 056012.
16. Hampson, R.E., Opris, I., Deadwyler, S.A., 2010. Neural correlates of fast pupil dilation in nonhuman primates: relation to behavioral performance and cognitive workload. *Behavioral Brain Research* 212, 1-11.
17. Hampson, R.E., Pons, T.P., Stanford, T.R., Deadwyler, S.A., 2004. Categorization in the monkey hippocampus: A possible mechanism for encoding information into memory. *Proc. Natl. Acad. Sci. U. S. A* 101, 3184-3189.
18. Hampson, R.E., Simeral, J.D., Berger, T.W., Song, D., Chan, R.H.M., Deadwyler, S.A., 2011. Cognitively relevant recoding in hippocampus: Beneficial feedback of ensemble codes in a closed loop paradigm. In: Vertes, R.P., Stackman, R.W. (Eds.), *Electrophysiological Recording Techniques Humana Press, New York*, pp. 215-240.
19. Hampson, R.E., Simeral, J.D., Deadwyler, S.A., 2005. Cognitive processes in replacement brain parts: A code for all reasons. In: Berger, T.W., Glanzman, D.L. (Eds.), *Toward Replacement Parts for the Brain. Implantable Biomimetic Electronics as Neural Prosthesis MIT Press, Cambridge, MA*, pp. 111-128.
20. Hampson, R.E., Simeral, J.D., Deadwyler, S.A., 2008. Neural population recording in behaving animals: Constituents of the neural code for behavior. In: Holscher, C., Munk, M.H. (Eds.), *Neural Population Encoding Cambridge University Press, Cambridge, UK*, pp. 74-94.
21. Hampson, R.E., Song, D., Chan, R.H., Sweatt, A.J., Riley, M.R., Gerhardt, G.A., Shin, D.C., Marmarelis, V.Z., Berger, T.W., Deadwyler, S.A., 2012. A nonlinear model for hippocampal cognitive prosthesis: memory facilitation by hippocampal ensemble stimulation. *IEEE Trans. Neural Syst. Rehabil. Eng* 20, 184-197.
22. Hampson, R.E., Song, D., Chan, R.H., Sweatt, A.J., Riley, M.R., Goonawardena, A.V., Marmarelis, V.Z., Gerhardt, G.A., Berger, T.W., Deadwyler, S.A., 2012. Closing the loop for memory prosthesis:

- detecting the role of hippocampal neural ensembles using nonlinear models. *IEEE Trans. Neural Syst. Rehabil. Eng* 20, 510-525.
23. Hampson, R.E., Song, D., Chan, R.H.M., Sweatt, A.J., Fuqua, J., Gerhardt, G.A., Shin, D., Marmarelis, V.Z., Berger, T.W., Deadwyler, S.A., 2012. A nonlinear model for hippocampal cognitive prostheses: Memory facilitation by hippocampal ensemble stimulation. *IEEE Transactions on Neural Systems and Rehabilitation Engineering*.
 24. Hampson, R.E., Song, D., Opris, I., Santos, L.M., Shin, D.C., Gerhardt, G.A., Marmarelis, V.Z., Berger, T.W., Deadwyler, S.A., 2013. Facilitation of memory encoding in primate hippocampus by a neuroprosthesis that promotes task-specific neural firing. *J Neural Eng* 10, 066013.
 25. Klausberger, T., Somogyi, P., 2008. Neuronal diversity and temporal dynamics: the unity of hippocampal circuit operations. *Science* 321, 53-57.
 26. Manns, J.R., Hopkins, R.O., Reed, J.M., Kitchener, E.G., Squire, L.R., 2003. Recognition memory and the human hippocampus. *Neuron* 37, 171-180.
 27. Marmarelis, V.Z., 2004. *Nonlinear Dynamic Modeling of Physiological Systems*. Wiley-IEEE Press, Hoboken, NJ.
 28. Marmarelis, V.Z., Berger, T.W., 2005. General methodology for nonlinear modeling of neural systems with Poisson point-process inputs. *Math. Biosci.* 196, 1-13.
 29. Marmarelis, V.Z., Orme, M.E., 1993. Modeling of neural systems by use of neuronal modes. *IEEE Trans. Biomed. Eng* 40, 1149-1158.
 30. Marmarelis, V.Z., Shin, D.C., Song, D., Hampson, R.E., Deadwyler, S.A., Berger, T.W., 2011. Dynamic nonlinear modeling of interactions between neuronal ensembles using principal dynamic modes. *Conf. Proc. IEEE Eng Med. Biol. Soc.* 2011, 3334-3337.
 31. Opris, I., Fuqua, J.L., Huettl, P.F., Gerhardt, G.A., Berger, T.W., Hampson, R.E., Deadwyler, S.A., 2012. Closing the loop in primate prefrontal cortex: inter-laminar processing. *Front Neural Circuits.* 6, 88.
 32. Opris, I., Hampson, R.E., Gerhardt, G.A., Berger, T.W., Deadwyler, S.A., 2012. Columnar processing in primate prefrontal cortex: Evidence for executive control microcircuits. *J. Cogn Neurosci.* 24, 2334-2347.
 33. Porrino, L.J., Daunais, J.B., Rogers, G.A., Hampson, R.E., Deadwyler, S.A., 2005. Facilitation of task performance and removal of the effects of sleep deprivation by an ampakine (CX717) in nonhuman primates. *PLoS. Biol.* 3, e299.

34. Quirk, G.J., Muller, R.U., Kubie, J.L., Ranck, J.B., Jr., 1992. The positional firing properties of medial entorhinal neurons: description and comparison with hippocampal place cells. *J. Neurosci.* 12, 1945-1963.
35. Riddle, D.R., Lichtenwalner, R.J., 2007. Neurogenesis in the Adult and Aging Brain. In: Riddle, D.R. (Ed.), *Brain Aging: Models, Methods, and Mechanisms (Frontiers in Neuroscience)* CRC Press, Boca Raton (FL).
36. Ross, R.S., Slotnick, S.D., 2008. The hippocampus is preferentially associated with memory for spatial context. *J. Cogn Neurosci.* 20, 432-446.
37. Rutishauser, U., Mamelak, A.N., Schuman, E.M., 2006. Single-trial learning of novel stimuli by individual neurons of the human hippocampus-amygdala complex. *Neuron* 49, 805-813.
38. Santos, L., Opris, I., Fuqua, J., Hampson, R.E., Deadwyler, S.A., 2012. A novel tetrode microdrive for simultaneous multi-neuron recording from different regions of primate brain. *J Neurosci. Methods* 205, 368-374.
39. Schwartz, A.B., Moran, D.W., Reina, G.A., 2004. Differential representation of perception and action in the frontal cortex. *Science* 303, 380-383.
40. Song, D., Chan, R.H., Marmarelis, V.Z., Hampson, R.E., Deadwyler, S.A., Berger, T.W., 2007a. Nonlinear dynamic modeling of spike train transformations for hippocampal-cortical prostheses. *IEEE Trans. Biomed. Eng* 54, 1053-1066.
41. Song, D., Chan, R.H., Marmarelis, V.Z., Hampson, R.E., Deadwyler, S.A., Berger, T.W., 2007b. Statistical selection of multiple-input multiple-output nonlinear dynamic models of spike train transformation. *Conf. Proc. IEEE Eng Med. Biol. Soc.* 2007, 4727-4730.
42. Song, D., Chan, R.H., Marmarelis, V.Z., Hampson, R.E., Deadwyler, S.A., Berger, T.W., 2009. Nonlinear modeling of neural population dynamics for hippocampal prostheses. *Neural Netw.* 22, 1340-1351.
43. Squire, L.R., Wixted, J.T., Clark, R.E., 2007. Recognition memory and the medial temporal lobe: a new perspective. *Nat. Rev. Neurosci.* 8, 872-883.
44. Truccolo, W., Eden, U.T., Fellows, M.R., Donoghue, J.P., Brown, E.N., 2005. A point process framework for relating neural spiking activity to spiking history, neural ensemble, and extrinsic covariate effects. *Journal of Neurophysiology* 93, 1074-1089.
45. Wais, P.E., Wixted, J.T., Hopkins, R.O., Squire, L.R., 2006. The hippocampus supports both the recollection and the familiarity components of recognition memory. *Neuron* 49, 459-466.

46. Wessberg, J., Stambaugh, C.R., Kralik, J.D., Beck, P.D., Laubach, M., Chapin, J.K., Kim, J., Biggs, S.J., Srinivasan, M.A., Nicolelis, M.A., 2000. Real-time prediction of hand trajectory by ensembles of cortical neurons in primates. *Nature* 408, 361-365.
47. Winters, B.D., Bussey, T.J., 2005. Transient inactivation of perirhinal cortex disrupts encoding, retrieval, and consolidation of object recognition memory. *J. Neurosci.* 25, 52-61.
48. Zanos, T.P., Courellis, S.H., Berger, T.W., Hampson, R.E., Deadwyler, S.A., Marmarelis, V.Z., 2008. Nonlinear modeling of causal interrelationships in neuronal ensembles. *IEEE Trans. Neural Syst. Rehabil. Eng* 16, 336-352.

ACCEPTED MANUSCRIPT

Figure Legends:

Figure 1: Illustration of DMS behavioral task and localization of hippocampal recording electrodes. **A:** Behavioral paradigm showing the sequence of events in the DMS task with correct cursor movement (yellow dot) indicated for each phase of the task: (1) Trial initiation ‘start signal’ (to maintain subject attention and signal the start of a new trial. Signal consists of yellow circle (upper) or blue square (lower) signaling an object or spatial trial, respectively. Placement of the cursor into the start signal initiated the Sample Phase of the trial. (2) Sample Presentation (SP) of a clip-art image in one of eight different spatial locations on the screen. The Sample Response (SR) consisted of movement of the cursor onto the presented sample image, which ended the Sample Phase and initiated the Delay Phase. (4) Variable Delay consisted of randomly-selected 1-60 sec interval with only a black screen showing. When computer determined that Delay interval had timed out, the Match Phase was initiated independent of any subject response. (5) Match Presentation (MP) consisted of display of Sample image in a different location from Sample Phase, along with 1-7 Non-match distracter images. Match response (MR) consisted of cursor movements onto same image (for Object trials, red arrow) or same position (for Spatial trials, blue arrow) as in the Sample Phase. (6) Correct MRs were rewarded by delivery of a squirt of juice reward (Reinf.). Placement of the cursor onto a non-match (distracter) image (object trial) or onto a different screen location from the SR (spatial trial) caused the screen to go blank without reward delivery. Inter-trial interval: 10.0 s. **B:** Overall performance averages showing the interaction of interposed delays with number of images presented in Match Phase. High and Low Cognitive Load conditions indicated by dashed outlines. **C:** Differential mean per cent correct performance in object and spatial trials (blue and red arrows in **A**) as a function of the number of (distracter) images presented in the match phase of the task. * $p < 0.01$, ** $p < 0.001$ Object vs. Spatial. **D:** Diagram of NHP brain in cross-section showing hippocampal tetrode tracks through temporal lobe and placement in the CA3 and CA1 cell layers.

Figure 2: Ensemble encoding of DMS task events. Heat maps depict trial-based firing of hippocampal CA1 and CA3 neural ensembles averaged across 100 DMS trials. Vertical axis depicts individual cells ($n=15$), while horizontal axis depicts elapsed time during typical DMS trials. DMS Sample Presentation (SP), Sample Response (SR), Match Presentation (MP) and Match Response (MR) are depicted on the horizontal axis by +1 and -1 sec brackets around each event and by vertical dashed lines. Trials were sorted according to Object vs. Spatial trials, and correct vs. error performance prior to averaging firing rate for each cell within the session. Mean firing rate is normalized to probability of firing across trials, at a temporal resolution of 100 ms, and represented by the color code scale at the bottom. Data shown is from a single subject/single ensemble recording session.

Figure 3: Hippocampal CA1 and CA3 neuron firing in the Sample and Match Phases of the DMS task. **A.** Trial-based histograms (TBHs) of average firing of all CA1 cells ($n= 431$) recorded during Sample Phase from all 4 NHPs performing the DMS task. Each trace represents one of the 4 conditions listed on the left for comparison of correct Object vs. Spatial trials. The three events in the Sample phase (Start = Strt, Sample Present = SP, Sample Response = SR) are listed on the x-axis and marked by vertical dotted lines on each TBH. **B.** TBHs for Match Phase recorded from the same CA1 neurons as in **A.** Note the sustained elevated mean firing rates from Match onset until reward delivery or trial termination. Match Presentation (MP) and Match Response (MR) are indicated on the x-axis and by vertical dashed lines. The brief firing peaks that occurred coincident with reinforcement (Reinf.) occurred after the MR primarily on Object trials. **C.** TBHs of average firing for all CA3 cells ($n= 801$) recorded during Sample Phase. **D.** Match Phase TBHs for same CA3 neurons graphs as in **C.** Note that CA3 and CA1 neurons exhibited similar responses to the DMS trial events indicated. Error bars indicated peak S.E.M. for each TBH.

Figure 4: Comparison of Sample and Match Phase peak firing for Correct and Error Object and Spatial trials. **A.** Plots of CA1 mean (\pm S.E.M.) peak responses to the same 3 events in the Sample phase shown in Figure 3A. Trials were sorted by Object and Spatial contingencies, for Correct vs. Error trials to show firing tendencies and differential encoding under different task

conditions including correct and error trials. **B.** Mean (\pm S.E.M.) peak responses for CA1 neurons during two Match Phase events (MP, MR), plus Reinforcement (Reinf) delivery phase. **C.** Mean (\pm S.E.M.) peak Sample Phase responses (Start, SP, SR) for CA3 cells. **D.** Mean (\pm S.E.M.) peak Match Phase responses (MP, MR, Reinf) for CA3 cells. Start = Start Signal = trial initiation, SP = Sample Presentation, SR = Sample Response, MP = Match Presentation, MR = Match Response. $*p<0.01$, $**p<0.001$ Object vs. Spatial trial peaks, $^{\#}p<0.01$, $^{\#\#}p<0.001$ Correct vs. Error trial peaks.

Figure 5: Multi-input, Multi-output (MIMO) nonlinear model used to: (a) calculate SR encoding via spatiotemporal firing relations between CA3 and CA1 recordings of neuron spike trains, (b) predict CA1 firing (c) from CA3 recordings (d), and generate patterned stimulation (e) for feedback stimulation of the same CA1 areas. The anatomical diagrams show placement of CA3 and CA1 multi-cell recording tetrodes in the respective areas along the longitudinal axis of hippocampus. Recordings on correct DMS trials from these spatially distinct and layer specific tetrodes were fed into the MIMO model with CA3 as the input (blue arrow) and CA1 as the output pattern (red arrow). The MIMO model predicted correct CA1 output firing (i.e. "Strong Codes") from CA3 inputs computed over the Sample Phase of the same trials (blue and red shaded rectangles) based on micro-temporal relationships between spike trains recorded at different spatial locations on correct trials. On stimulation trials, trains of electrical pulses mimicking the predicted Strong Code CA1 output spike trains were delivered to the same hippocampal electrode locations where the CA1 patterns were previously recorded. MIMO model stimulation patterns applied to the respective CA1 recording locations consisted of multi-channel biphasic pulses of 10-50 μ A, 1.0 ms duration with a minimum 50 ms between pulses, at ≤ 20 stimulation pulses per second per channel. [Figure from (Hampson et al., 2013), used with permission.]

Figure 6: Strong Sample Phase encoding extracted as a function of input-output relations of CA3 and CA1 firing on correct trials. The MIMO model was calculated using correct trials only for Object (left columns) and Spatial (right columns) trials, and yielded predictions of "Strong"

(i.e. most likely to be correct) Sample codes for each of four NHPs tested (rows, NHP 1-4). Heat maps depict firing probability arranged as a spatio-temporal pattern of CA1 neurons (vertical axis) by time (horizontal axis) starting at Sample Presentation (SP) and extending for two seconds, including the occurrence of the Sample Response (SR). Strong code stimulation patterns (left side of each pair) were delivered whenever the MIMO-extracted CA1 firing was predicted to consist of a "Weak" code (right side of each pair). The Heat-map color shows a code for spike train firing probability (as predicted by MIMO model) ranging from < 10% (dark blue) to $\geq 80\%$ (red). Note that Weak code firing often shows lower probability of firing, but a similar spatio-temporal pattern to the Strong codes for the opposite trial type (i.e. Object vs. Spatial trial).

Figure 7: Facilitation of DMS task performance in four nonhuman primates (NHPs 1-4) following delivery of MIMO strong codes (Figure 5b) via CA1 hippocampal stimulation derived from prior correct responses in previous sessions. Each graph shows the difference in performance for each of the 4 subjects on randomly selected stimulation trials vs. nonstimulated trials as a function of duration of the number (#) of distracter images (or intervening delay, insets). Strong code stimulation patterns (Stim, red traces) were delivered to CA1 hippocampal areas in the Sample phase on 40-50 of the different trial types during the same sessions in which 80-100 non-stimulated trials (No Stim, blue traces) were also assessed on similar types of trials. Data in the above performance graphs were from 4 sessions per NHP subject. $*p < 0.01$, $**p < 0.001$ Stim vs. No Stim.

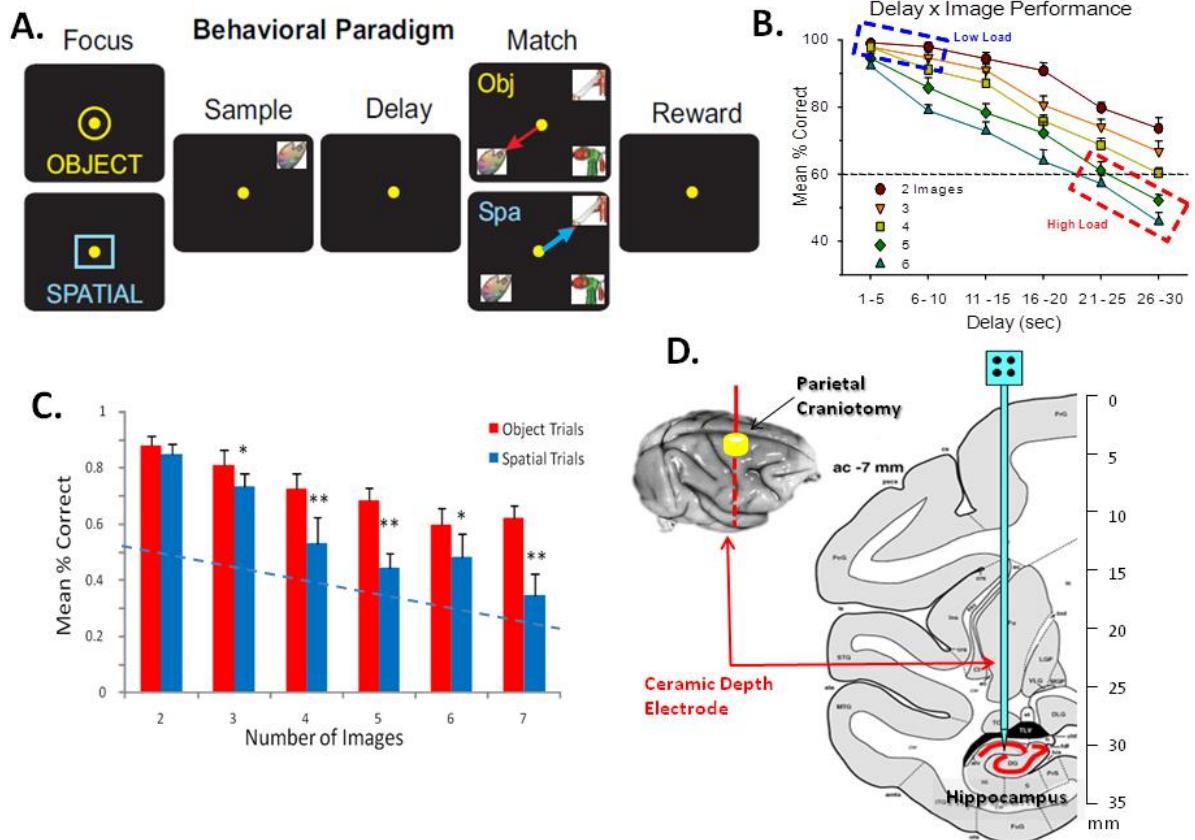


Figure 1

ACCEPTED

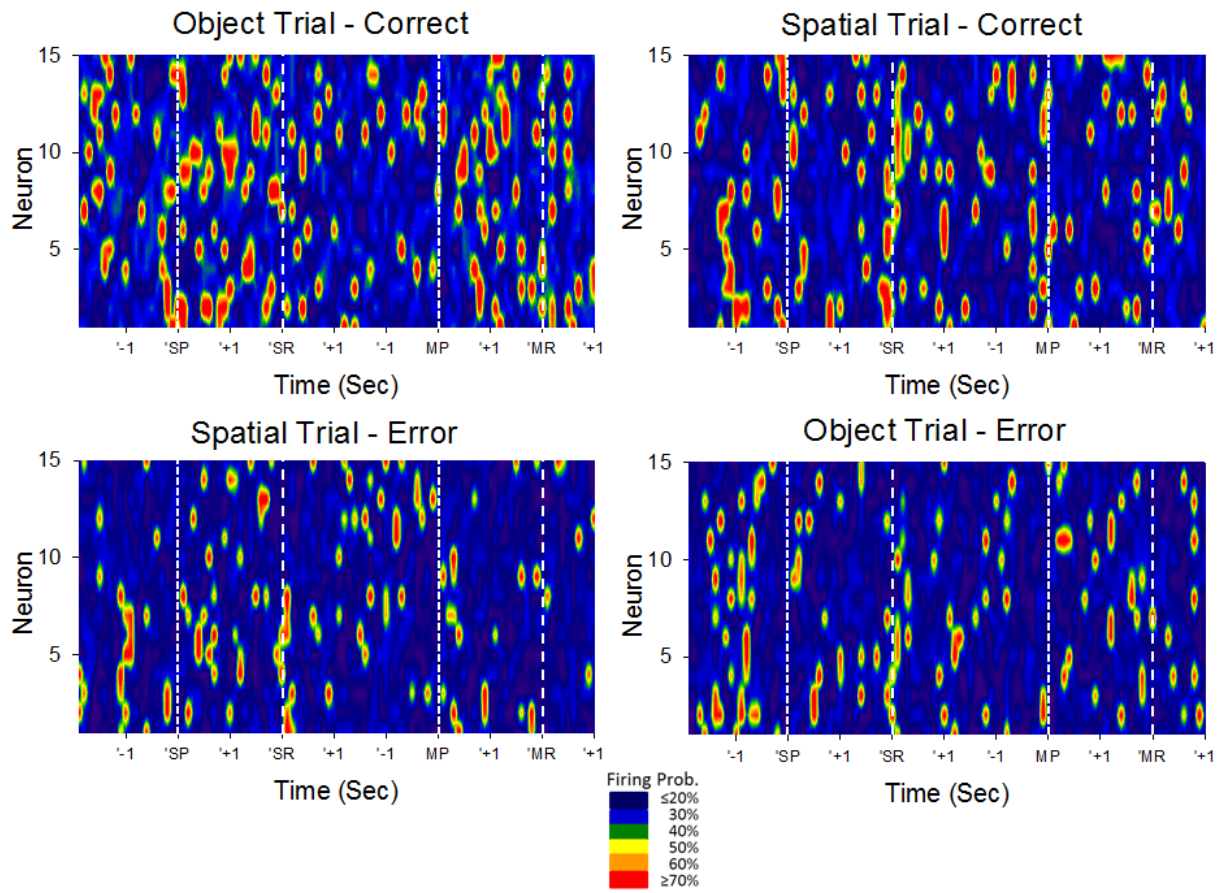


Figure 2

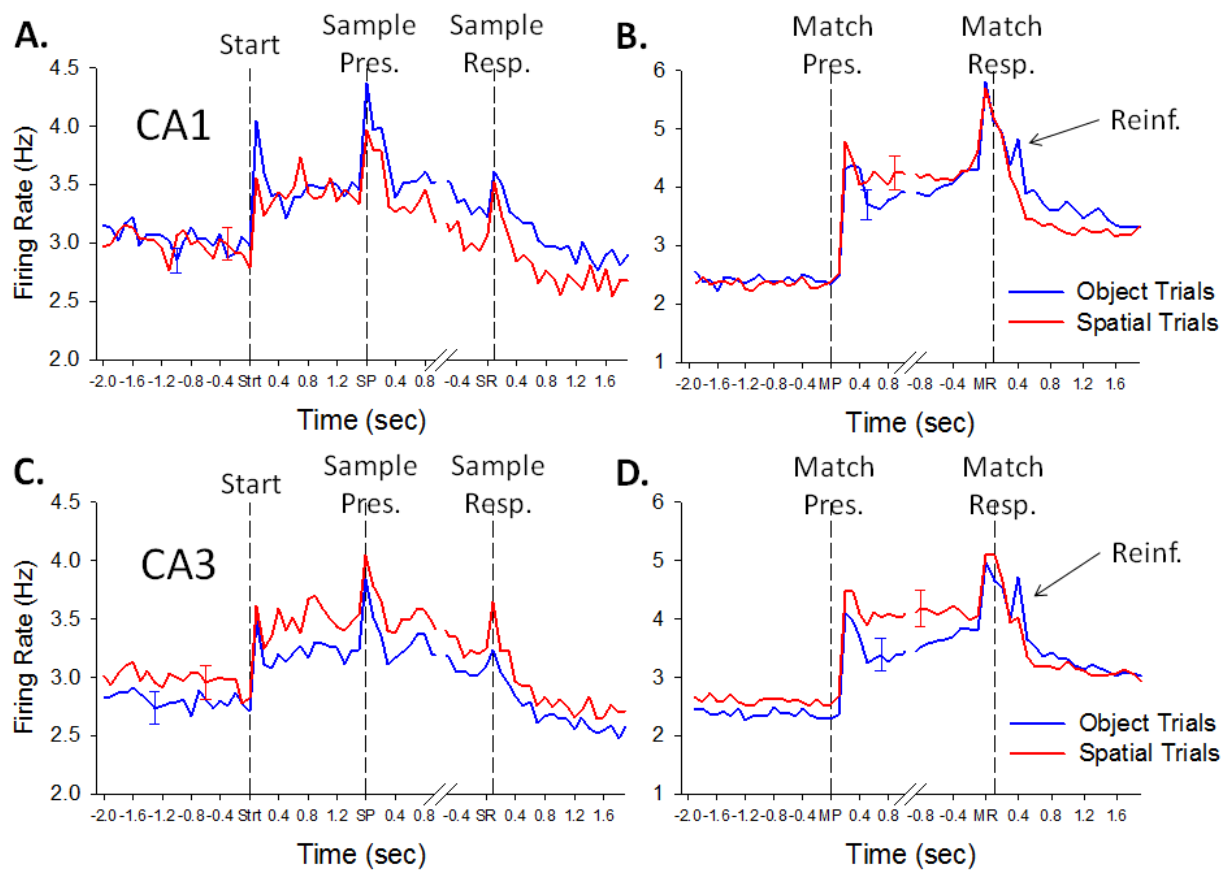


Figure 3

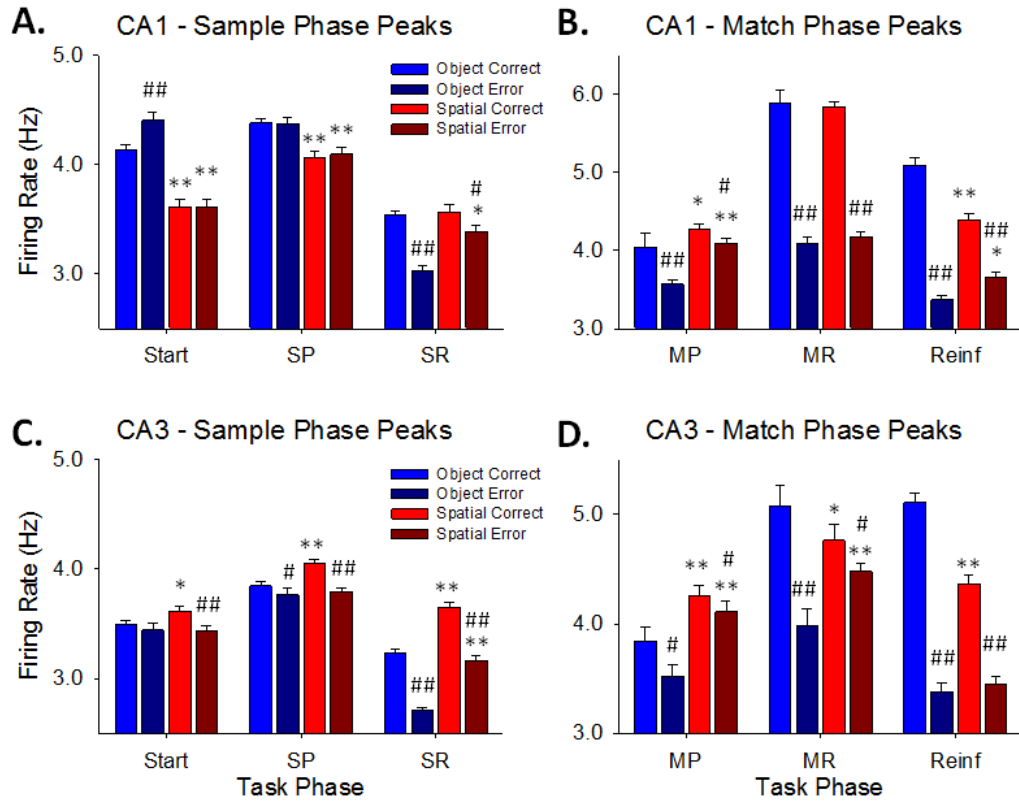


Figure 4

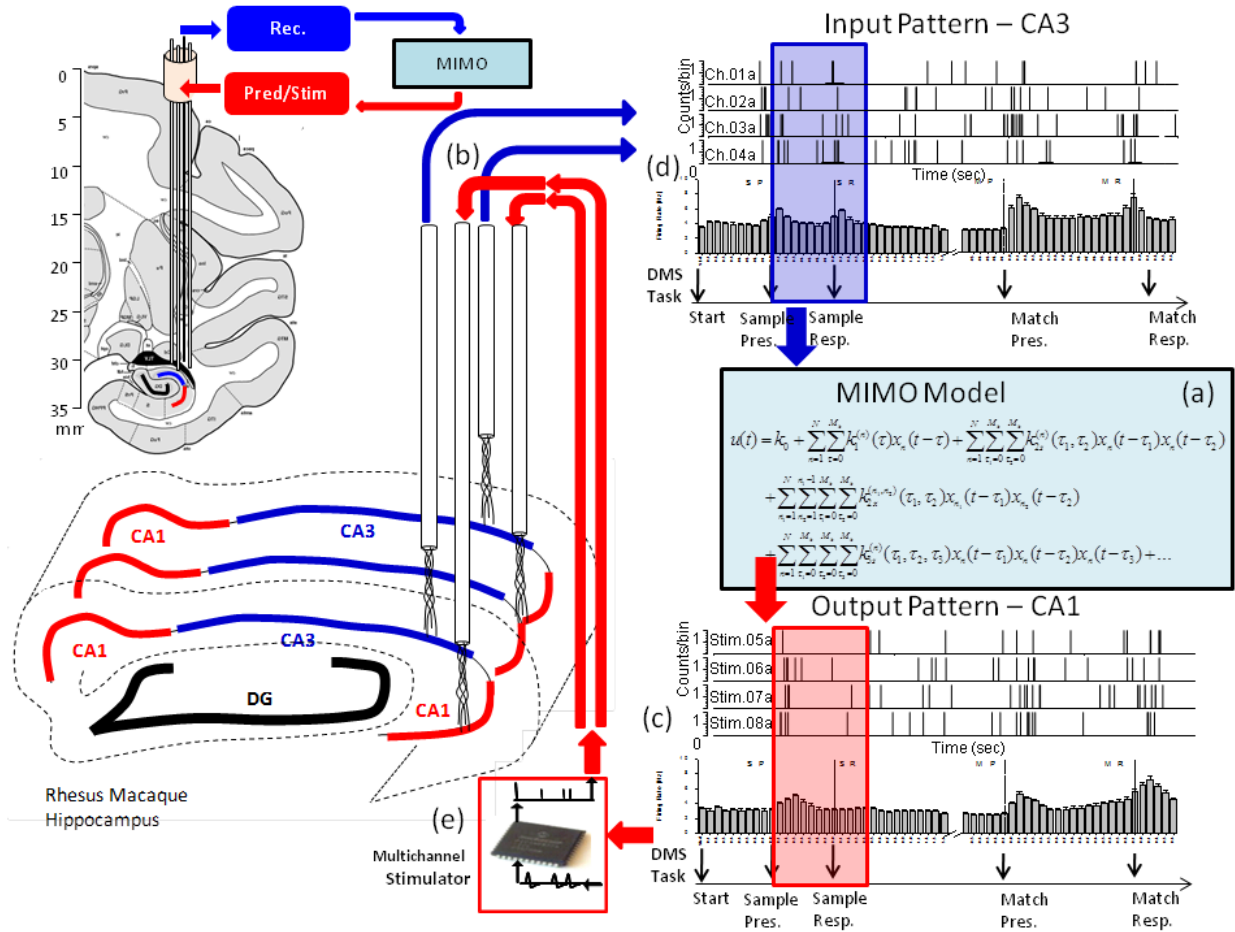


Figure 5

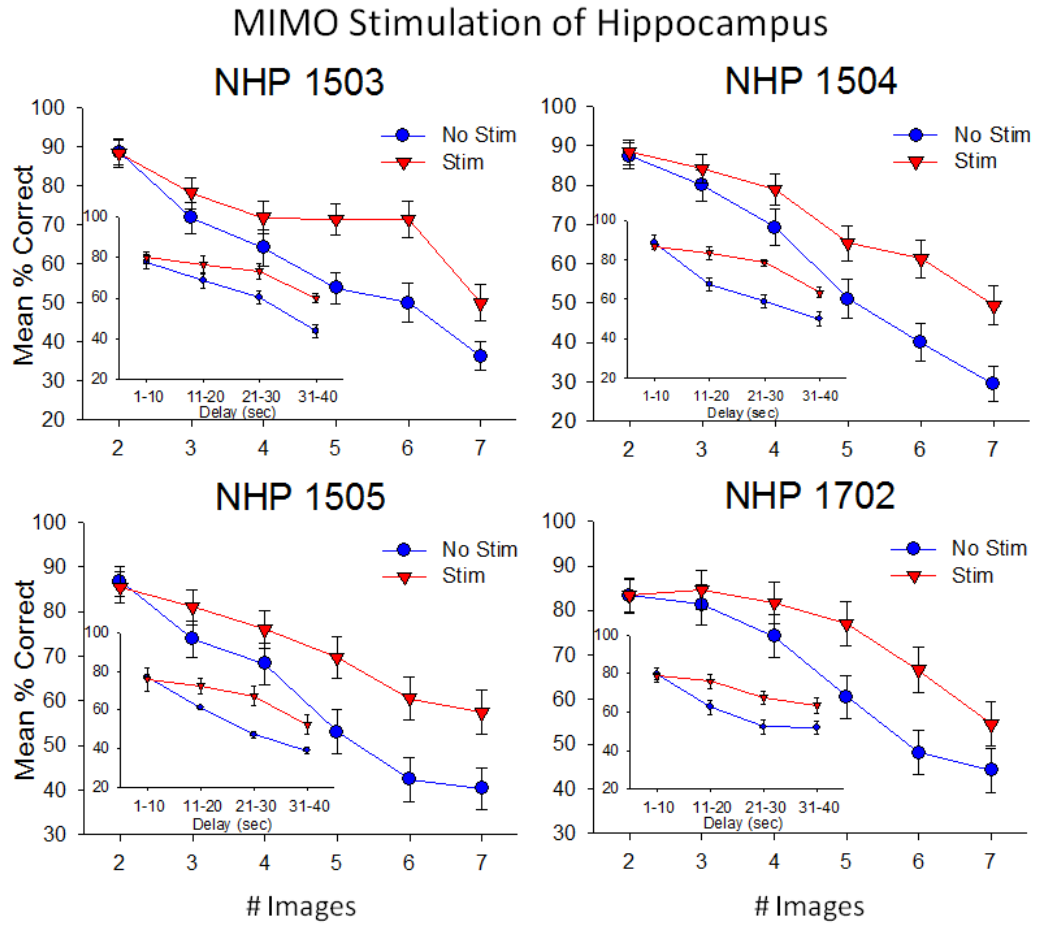


Figure 7

Highlights:

- **Analysis of hippocampal neural ensembles reveals unique codes for memory**
- **Nonlinear analysis of ensemble codes can predict correct or erroneous behaviors**
- **Electrical microstimulation of CA1 neurons can facilitate behavior and reduce errors**
- **Results provide a proof-of-concept for a prosthetic to restore human memory**

ACCEPTED MANUSCRIPT